Redox Biology 27 (2019) 101224

Contents lists available at ScienceDirect

Redox Biology

journal homepage: www.elsevier.com/locate/redox

Research Paper

Loss of GTPase activating protein neurofibromin stimulates paracrine cell communication via macropinocytosis

Pushpankur Ghoshal[a], Bhupesh Singla[a], Huiping Lin[a], Mary Cherian-Shaw[a], Rebekah Tritz[a], Caleb A. Padgett[a], Farlyn Hudson[a], Hanfang Zhang[a], Brian K. Stansfield[a,c], Gábor Csányi[a,b,*]

[a] Vascular Biology Center, Augusta University, Medical College of Georgia, Augusta, GA, 30912, USA
[b] Department of Pharmacology and Toxicology, Augusta University, Medical College of Georgia, Augusta, GA, 30912, USA
[c] Department of Pediatrics and Neonatal-Perinatal Medicine, Augusta University, Medical College of Georgia, Augusta, GA, 30912, USA

ARTICLE INFO

Keywords:
Neurofibromin
Macropinocytosis
NADPH oxidase
Macrophages and exosomes

ABSTRACT

Neurofibromin, the protein product of the neurofibromatosis type 1 (*NF1*) tumor suppressor gene, is a negative regulator of Ras signaling. Patients with mutations in *NF1* have a strong predisposition for cardiovascular disease, which contributes to their early mortality. *Nf1* heterozygous ($Nf1^{+/-}$) bone marrow to wild type chimeras and mice with heterozygous recombination of *Nf1* in myeloid cells recapitulate many of the vascular phenotypes observed in $Nf1^{+/-}$ mutants. Although these results suggest that macrophages play a central role in NF1 vasculopathy, the underlying mechanisms are currently unknown. In the present study, we employed macrophages isolated from either $Nf1^{+/-}$ or Lysm $Cre^{+}/Nf1^{f/f}$ mice to test the hypothesis that loss of *Nf1* stimulates macropinocytosis in macrophages. Scanning electron microscopy and flow cytometry analysis of FITC-dextran internalization demonstrated that loss of *Nf1* in macrophages stimulates macropinocytosis. We next utilized various cellular and molecular approaches, pharmacological inhibitors and genetically modified mice to identify the signaling mechanisms mediating macropinocytosis in *Nf1*-deficient macrophages. Our results indicate that loss of *Nf1* stimulates PKCδ-mediated $p47^{phox}$ phosphorylation via RAS activation, leading to increased NADPH oxidase 2 activity, reactive oxygen species generation, membrane ruffling and macropinocytosis. Interestingly, we also found that *Nf1*-deficient macrophages internalize exosomes derived from angiotensin II-treated endothelial cells via macropinocytosis *in vitro* and in the peritoneal cavity *in vivo*. As a result of exosome internalization, *Nf1*-deficient macrophages polarized toward an inflammatory M1 phenotype and secreted increased levels of proinflammatory cytokines compared to controls. In conclusion, the findings of the present study demonstrate that loss of *Nf1* stimulates paracrine endothelial to myeloid cell communication via macropinocytosis, leading to proinflammatory changes in recipient macrophages.

1. Introduction

Neurofibromatosis type 1 (NF1), also known as von Recklinghausen disease, is an autosomal dominant disorder affecting 1 in 3000 individuals [1]. NF1 results from mutations in the *NF1* tumor suppressor gene, which encodes the protein neurofibromin [2]. Neurofibromin functions as a GTP-ase activating protein (GAP) that negatively regulates RAS activity by accelerating the hydrolysis of active GTP-Ras [3]. As a consequence, inactivating mutations in *NF1* lead to enhanced RAS activity and downstream activation of phosphatidylinositol 3-kinase (PI3K)/Akt and MEK/ERK signaling pathways, resulting in a proliferating and prosurvival cellular phenotype [4]. The most common clinical manifestations of NF1 include dermal and plexiform neurofibromas and various non-malignant manifestations, including learning deficits, skeletal abnormalities and cardiovascular disease [5].

Cardiovascular abnormalities are relatively common, but underappreciated complications of NF1, contributing to increased morbidity and mortality, particularly among younger patients [6,7]. The vascular complications of NF1 include arterial stenosis, systemic hypertension, aneurysm formation and cerebrovascular disease [5]. The pathophysiology of NF1 vasculopathy is not well understood, although recent studies using $Nf1^{+/-}$ mice have shed some light on the possible cellular mechanisms. Li et al. showed that heterozygous inactivation of *Nf1* increases angiotensin II (AngII)-induced aneurysm formation and reactive oxygen species (ROS) generation in the abdominal aorta compared with wild type mice [8]. Another study demonstrated that $Nf1^{+/}$

* Corresponding author. CB-3213A, 1459 Laney Walker Blvd., Augusta University, Medical College of Georgia, Augusta, GA, 30912, USA.
E-mail address: gcsanyi@augusta.edu (G. Csányi).

https://doi.org/10.1016/j.redox.2019.101224
Received 28 December 2018; Received in revised form 26 April 2019; Accepted 16 May 2019
Available online 30 May 2019

Abbreviations:

AKT	Protein kinase B
BMDM	Bone marrow-derived macrophages
DCFH-DA	Dichloro-dihydro-fluorescein diacetate
EIPA	5-(N-Ethyl-N-isopropyl)amiloride
EC	Endothelial Cells
M-CSF	Macrophage colony-stimulating factor
MSC	Mesenchymal stem cells
Nf1	Neurofibromatosis type 1 gene
Nf1 $^{+/-}$	Global *Nf1* heterozygous knockout mice
Nf1$^{f/f}$	*floxed Nf1* mice
NOS	Nitric oxide synthase
Nox2	NADPH oxidase 2
$O_2^{\cdot-}$	Superoxide anion
PI3K	Phosphatidylinositide 3-kinase
Ras	p21Ras pathway
ROS	Reactive oxygen species
SOD	Superoxide dismutase
SEM	Scanning Electron Microscopy
TEM	Transmission Electron Microscopy
WT	Wild type

$^{-}$ mice have increased neointima formation in response to arterial injury [9]. Interestingly, adoptive transfer of bone marrow-derived cells from *Nf1*$^{+/-}$ mice to wild type mice and heterozygous deletion of *Nf1* in myeloid cells alone recapitulated vascular phenotype observed in *Nf1*$^{+/-}$ mice [8,9]. These results are somewhat surprising as previous studies have demonstrated a complex interaction between vascular cells and leukocytes in the pathogenesis of neointima formation, arterial stenosis and aneurysm development in non-NF1 models [10]. In support of the role of macrophages in NF1-associated pathologies in humans, previous studies have demonstrated that NF1 patients have increased levels of proinflammatory monocytes ($CD14^+CD16^{++}$) in the peripheral blood compared with age- and sex-matched controls. Further, inflammatory macrophages accumulate in plexiform neurofibromas and appear to support their growth and malignant potential [11,12]. Similar to NF1 patients, *Nf1*$^{+/-}$ mice have increased circulating proinflammatory ($Ly6C^{hi}CCR2^+$) monocytes and increased arterial accumulation of macrophages in an AngII model of aneurysm formation and in response to mechanical injury [8,9,11]. Taken together, these results suggest an important role for macrophages in the pathogenesis of NF1 vasculopathy, yet the mechanisms by which neurofibromin-deficient macrophages contribute to the development of vascular disorders remain unknown.

Macropinocytosis is an actin-driven process of large-scale, non-specific fluid uptake used for feeding by some cancer cells and eukaryotic bacterivores and antigen sampling by immune cells [13–15]. In mammalian cells and *Dictyostelium*, active Ras, PI3K, D-3 phosphorylated phosphatidylinositols, protein kinase C (PKC) and actin are important signaling molecules required for efficient fluid-phase macropinocytosis [16–18]. Interestingly, a previous study using whole genome sequencing identified that axenic *Dictyostelium* carrying inactivating mutations in *Nf1* have stimulated macropinocytosis, leading to increased nutrient internalization and their robust proliferation [19]. Increasing evidence supports the hypothesis that macropinocytosis contributes to cancer propagation and the development of cardiovascular disorders [13,20,21]. Incidentally, cancer and vascular abnormalities, the two most frequent complications of NF1, are major contributors to the decreased life expectancy (~15 years) of patients with NF1 [7]. However, whether neurofibromin regulates macropinocytosis in macrophages or any mammalian cells, and how neurofibromin controls the regulatory pathways that mediate macropinocytosis to support macrophage-linked cardiovascular disease reminiscent of the NF1 phenotype remain unknown.

In the present study, we employed macrophages isolated from either *Nf1*$^{+/-}$ or Lysm Cre^+/*Nf1*$^{f/f}$ mice to test the hypothesis that loss of neurofibromin stimulates macropinocytosis in mammalian cells. Our results demonstrate that loss of neurofibromin stimulates macrophage macropinocytosis *in vitro* and *in vivo*. Mechanistically, we found that neurofibromin-deficiency stimulates PKCδ-mediated $p47^{phox}$ phosphorylation via RAS activation, leading to increased NADPH oxidase 2 (Nox2) activity, ROS generation, membrane ruffling and macropinocytosis. Interestingly, we also found that neurofibromin-deficient macrophages internalize exosomes derived from AngII-treated endothelial cells via macropinocytosis. As a result, neurofibromin-deficient macrophages tend to polarize toward an inflammatory M1 phenotype and secrete proinflammatory cytokines. Taken together, these findings may contribute to a better understanding of how NF1-associated vascular disorders develop and inform new therapeutic strategies for the vascular complications of this human disease. The current data are also expected to stimulate new inquiries into neurofibromin-mediated macropinocytosis in other cell types, including Schwann cells, and may lead to broader areas of exploration investigating the role of macropinocytosis in the malignant complications of NF1.

2. Materials and methods

2.1. Reagents

EUK-134, DPI, LY294002, calphostin C, 5-(N-Ethyl-N-isopropyl) amiloride (EIPA), cytochalasin D, FITC-dextran, DCFH-DA, PKH67 kit and thioglycollate medium were purchased from Sigma-Aldrich (St. Louis, MO, USA). M-CSF was purchased from Miltenyi Biotec Inc. (San Diego, CA, USA). The antibody array kit was obtained from RayBiotech. Phospho-PKCδ (Tyr-311), phospho-ERK (Tyr 204), β–tubulin and total ERK antibodies were obtained from Cell Signaling Technology (Danvers, MA, USA). Phospho-$p47^{phox}$ was obtained from Sigma-Aldrich (St. Louis, MO, USA). Nox2 antibody was obtained from Abcam. Total PKCδ, NOS2, arginase 1 and anti-β-actin antibodies were procured from Santa Cruz Biotechnology (Dallas, TX, USA).

2.2. Animals

Animal experiments were approved by the Laboratory Animal Services at Augusta University. *Nf1*$^{+/-}$ mice were kindly provided by Tyler Jacks (MIT, Boston, MA) and LysM Cre mice were purchased from the Jackson Laboratory. *Nf1*$^{flox/flox}$ mice were obtained from Luis Parada (University of Texas Southwestern Medical Center, Dallas, TX). All mice were maintained on the C57BL/6 background. *Nf1*$^{flox/flox}$ mice were crossed with LysM Cre mice to generate littermate Cre^+ and Cre^- *Nf1*$^{flox/flox}$ mice. Cre-mediated recombination was confirmed by PCR as previously described [11]. The following primers were used for genotyping; Cre: TTA CAG TCG GCC AGG CTG AC, CTT GGG CTG CCA GAA TTT CTC and CCC AGA AAT GCC AGA TTA CG; Lox: TGA TTC CCA CTT TGT GGT TCT AAG, CTT CAG ACT GAT TGT TGT ACC TGA and ACC TCT CTA GCC TCA GGA ATG A. For genotyping *Nf1*$^{+/-}$ mice, we used the following primers: CAC CTT TGT TTG GAA TAT ATG ACT, ATT CGC CAA TGA CAA GAC and TTC AAT ACC TGC CCA AGG.

2.3. Cell culture

Bone marrow-derived monocytes and thioglycollate-elicited peritoneal macrophages were cultured in Roswell Park Memorial Institute (RPMI) 1640 medium (without 2-mercaptoethanol) containing 10% fetal bovine serum (FBS) and supplemented with a 1% antibiotic

solution containing penicillin and streptomycin (Thermo Fisher Scientific, Waltham, MA, USA). Bone marrow-derived monocytes were differentiated into macrophages using murine M-CSF (20 ng/mL,9 days) as reported previously [22]. After treatment, adherent cells were trypsinized and seeded in new cell culture plates in RPMI medium without M-CSF. Cells were used for experiments after overnight incubation.

2.4. Flow cytometry

Bone marrow-derived macrophages (BMDM) were treated with FITC-dextran (70,000 MW, 150 μg/mL) for 2, 4 or 16 h in the presence or absence of the inhibitors as described. Cells were washed twice with ice-cold PBS, fixed in 2% paraformaldehyde (PFA), resuspended in FACS buffer (2% BSA and 0.01% sodium azide in PBS) and analyzed for FITC-dextran uptake using flow cytometry (Ex: 488 nm, Em: 530 nm). Mean fluorescence intensity was used to compare FITC-dextran internalization among the groups. All FACS experiments were performed using the Becton Dickinson FACS Calibur and BD accuri C6 flow cytometer.

2.5. Confocal microscopy

Macrophages were fixed in 2% paraformaldehyde (PFA), permeabilized with 0.1% Triton X-100, and stained with Hoechst 33342 (Life Technologies, NY, USA). Images were taken with a Zeiss 780 inverted confocal microscope.

2.6. Scanning electron microscopy

Macrophages were fixed (4% paraformaldehyde, 2% glutaraldehyde in 0.1 M sodium cacodylate solution) overnight at 4 °C. Then cells were dehydrated through a graded ethanol series (25%–100%) and washed with 100% ethanol before critical point drying (Tousimis Samdri-790, Rockville, MD). Coverslips were mounted onto aluminum stubs and sputter coated with 3.5 nm of gold/palladium (Anatek USA-Hummer, Union City, CA). Cell were imaged at 20 KV using a Philips XL30 scanning electron microscope (FEI, Hillsboro, OR.) The number of ruffles on the surface of $Cre^{-}/Nf1^{f/f}$ and $Cre^{+}/Nf1^{f/f}$ macrophages were visually quantified and normalized to total cell number.

2.7. Transmission electron microscopy

TEM sample preparation and imaging was performed at the Electron Microscopy and Histology Core Laboratory at Augusta University (www.augusta.edu/mcg/cba/emhisto/).

2.8. L-012 chemiluminescence

L-012 chemiluminescence to measure superoxide anion ($O_2^{\bullet -}$) generation was described previously [23]. Cells (50,000/well) were plated in white 96 well plates in sterile phosphate-buffered saline (PBS) containing L-012 (400 μM; Wako Chemicals, USA). Chemiluminescence was measured at 37 °C using a Lumistar Galaxy (BMG) luminometer.

2.9. DCFH fluorescence

Intracellular ROS were measured using 2′, 7′-dichloro-dihydrofluorescein diacetate (DCFH-DA). Briefly, macrophages were seeded in six well plates at a density of 1×10^6 cells/well. After overnight incubation, cells were pre-incubated with a cell permeable antioxidant (EUK134, 10 μM, 1 h) or treated with vehicle. The cells were then treated with DCFH-DA (5 μM) at 37 °C for 30 min followed by flow cytometry analysis. H_2O_2 (0.1 mM) was used as a positive control.

2.10. Western blot

Cells were lysed in RIPA buffer (Pierce Biotechnology, Rockford, Illinois, USA). Protein concentration of supernatant was estimated using the bicinchoninic acid (BCA) protein assay (Pierce Biotechnology, Rockford, Illinois, USA), according to the manufacturer's instructions. Equal amounts of protein (30 μg) were separated by use of SDS-polyacrylamide gel electrophoresis (SDS-PAGE) and transferred to nitrocellulose membranes (Li-Cor Biosciences, Lincoln, NE, USA). The membranes were blocked and probed with primary antibodies followed by IRDye-conjugated secondary antibody treatment (Li-Cor Biosciences). Anti-β-actin antibody was used as a loading control.

2.11. Immunoprecipitation

Immunoprecipitation was performed as described previously [24]. Briefly, cell lysates were immunoprecipitated with a $p47^{phox}$ antibody (Santa Cruz Biotechnology, Dallas, TX, USA) overnight at 4 °C. The immunocomplexes were collected by washing six times with lysis buffer, boiled in 1 × Laemmli sample buffer (Bio-Rad) for 10 min and subjected to Western blot analysis with an anti-Nox2 antibody (Abcam).

2.12. Exosome preparation and characterization

Exosomes were collected by density gradient ultracentrifugation as described previously [25]. Briefly, endothelial cells were incubated for 48 h in complete medium (Promocell) with 10% exosome–depleted FBS (SBI, CA). The supernatant was collected and centrifuged at 800 × *g* for 10 min, followed by a centrifugation step of 3000 × *g* for 30 min to remove cell debris. After filtering with a 0.22-μm filter (Millipore), the exosomes were pelleted by ultracentrifugation at 100,000 × *g* for 2 h and re-suspended in PBS. The secreted microvesicles were characterized by Western blot using antibodies for the following exosome-specific markers: CD63 and CD81 (SBI, CA). Transmission electron microscopy (TEM) followed by CD63 labeling was performed at the Augusta University Imaging Core Facility. For exosome internalization experiments, exosomes were labeled with PKH67 Fluorescent Cell Linker Kits (Sigma-Aldrich) according to the manufacturer's instructions.

2.13. Mouse cytokine array analysis

Cytokine secretion was quantified using the mouse inflammation antibody array C1 (RayBiotech, USA). Briefly, LysM $Cre^{+}/Nf1^{f/f}$ and LysM $Cre^{-}/Nf1^{f/f}$ macrophages were treated for 48 h with or without exosomes. Cell culture media were collected and concentrated using ultra centrifugal filter units (10,000 MW cut, Amicon, Millipore) and stored at −80 °C for future use. Arrays were performed according to the instructions provided by RayBiotech using 500 μl supernatant. Average pixel intensity was quantified using ImageJ.

2.14. Statistical analysis

Statistical analysis was performed using GraphPad Prism (La Jolla, CA, USA). The data are expressed as mean ± SD/SEM. Student's t-test and one or two-way ANOVA were used as appropriate for the particular experiment and treatment groups. *P* values less than 0.05 were considered statistically significant.

3. Results

3.1. Neurofibromin deficiency stimulates fluid-phase macropinocytosis in macrophages

A previous study showed that loss of *Nf1* in *Dictyostelium* amoebae potentiates liquid and nutrient macropinocytosis, leading to stimulated axenic growth [19]. The signaling mechanisms, however, by which

neurofibromin deficiency stimulates macropinocytosis and whether neurofibromin regulates macropinocytosis in mammalian cells are unknown. As internalization of extracellular fluid and its solute is characteristic of macropinocytosis, we first examined whether loss of *Nf1* stimulates uptake of fluorescently-labeled dextran [FITC-dextran (70,000 MW), 150 μg/mL] in murine macrophages. For these experiments, bone marrows were harvested from LysM Cre^{+}/*Nf1*$^{flox/flox}$ and LysM Cre^{-}/*Nf1*$^{flox/flox}$ mice and monocytes were differentiated into macrophages using M-CSF (20 ng/mL, 9 days) [22]. BMDM were serum starved overnight to minimize exogenous macropinocytosis stimulation by cytokines and growth factors. As shown in Fig. 1A and B, BMDM isolated from LysM Cre^{+}/*Nf1*$^{flox/flox}$ mice internalized significantly more FITC-dextran compared to LysM Cre^{-}/*Nf1*$^{flox/flox}$ controls ($^{*}p < 0.05$; $n = 13$). A comparison of fluid uptake between LysM Cre^{+}/*Nf1*$^{flox/flox}$ and LysM Cre^{-}/*Nf1*$^{flox/flox}$ BMDM after shorter (2 and 4 h) and longer (16 h) incubation times is shown in Fig. S1. Similarly, FACS analysis confirmed a higher rate of FITC-dextran internalization in thioglycollate-elicited peritoneal macrophages isolated from LysM Cre^{+}/*Nf1*$^{flox/flox}$ mice when compared with Cre^{-} controls (Fig. 1C). Consistent with these results, macrophages isolated from *Nf1*$^{+/-}$ mice also demonstrated increased FITC-dextran incorporation when compared with wild type macrophages (Fig. 1D). The genotype of global and myeloid cell-specific knockout mice was confirmed by PCR analysis of genomic DNA (Supplementary Fig. S2) [26].

Plasma membrane ruffling initiated by submembranous activation of the actin cytoskeleton and its outward-directed polymerization is the first morphological step leading to macropinocytosis. Scanning electron microscopy (SEM) imaging demonstrated that neurofibromin-deficient macrophages exhibit marked cell surface ruffling compared to control cells (Fig. 1E). Both sheet-like membrane projections (yellow arrow) and fully formed (5–10 μm in diameter) C-shaped ruffles (red arrow) were visualized on the dorsal surface of LysM Cre^{+}/*Nf1*$^{flox/flox}$ macrophages. Quantification of membrane ruffles revealed a significant increase in membrane ruffling in *Nf1* knockout macrophages when compared with control macrophages (0.3 ± 0.1 and 4.9 ± 1; for LysM Cre^{-}/*Nf1*$^{flox/flox}$ and LysM Cre^{+}/*Nf1*$^{flox/flox}$ macrophages, respectively; $^{*}p < 0.05$).

Macropinocytosis is pharmacologically defined by its sensitivity to inhibitors of Na^{+}/H^{+} exchanger (NHE) [27] and actin polymerization [28]. Therefore, we examined the effect of the NHE blocker EIPA (10 μM, 30 min) and actin perturbant cytochalasin D (1 μM, 30 min) on FITC-dextran internalization by NF1-deficient macrophages. Fig. 1F shows that EIPA and cytochalasin D completely abolished FITC-dextran uptake in LysM Cre^{+}/*Nf1*$^{flox/flox}$ macrophages, consistent with the uptake mediated by macropinocytosis. A recent study by our group demonstrated that imipramine, an FDA-approved tricyclic antidepressant, potently inhibits macropinocytosis without blocking phagocytosis, clathrin- or caveolin mediated endocytosis [26]. As shown in Fig. 1G, pretreatment of NF1-deficient macrophages with imipramine (5 μM, 30 min) blocked FITC-dextran internalization. Next, we quantified

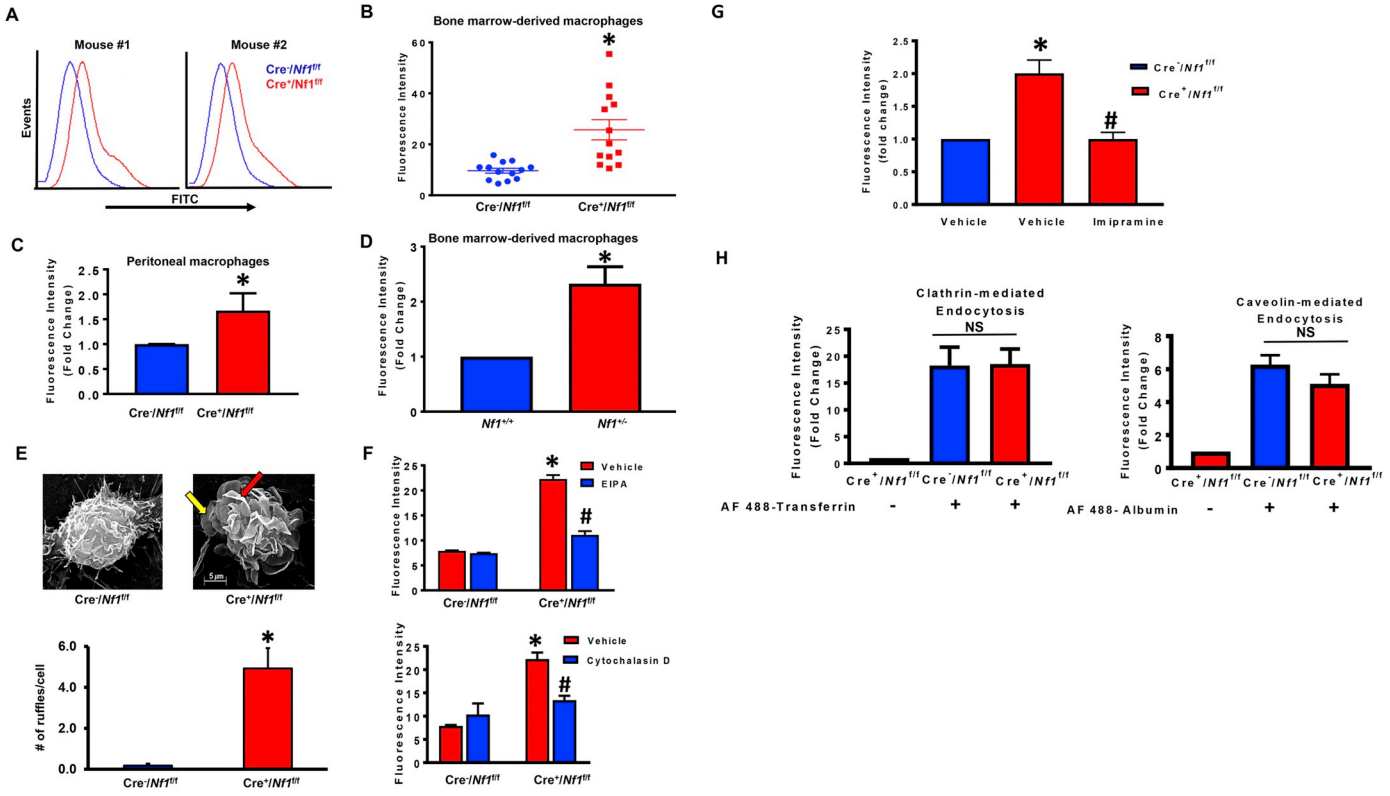

Fig. 1. Loss of NF1 function stimulates fluid-phase macropinocytosis in macrophages. **(A)** Representative FACS histograms illustrating FITC–dextran accumulation by bone marrow derived macrophages from LysM Cre^{+}/*Nf1*$^{flox/flox}$ mice (red) compared to LysM Cre^{-}/*Nf1*$^{flox/flox}$ mice (blue). Cells were incubated with FITC-dextran (150 μg/mL) for 16 h followed by FACS analysis. **(B)** Comparison of fluorescence intensity quantification of flow data between LysM Cre^{-} *Nf1*$^{flox/flox}$ and LysM Cre^{+}/*Nf1*$^{flox/flox}$ BMDM ($n = 13$) **(C)**. FACS analysis of FITC-dextran uptake in peritoneal LysM Cre^{+}/*Nf1*$^{flox/flox}$ macrophages compared with Cre^{-} controls ($n = 3$). **(D)** FITC-dextran incorporation into *Nf1*$^{+/-}$ macrophages compared with wild type cells ($n = 4$). **(E)** *Upper panel:* representative images of scanning electron microscopy (SEM). *Lower panel* demonstrates quantification of membrane ruffles on the surface of LysM Cre^{-}/*Nf1*$^{flox/flox}$ and LysM Cre^{+}/*Nf1*$^{flox/flox}$ BMDM ($n = 3$). **(F)** Cells were treated with vehicle, EIPA (10 μM, 30 min) or cytochalasin D (1 μM, 30 min) followed by FITC-dextran administration (16 h). FITC fluorescence was analyzed by FACS ($n = 3$). **(G)** Quantification of FITC-dextran accumulation by BMDM from LysM Cre^{+} *Nf1*$^{flox/flox}$ compared with LysM Cre^{-}/*Nf1*$^{flox/flox}$ mice pretreated with ± imipramine (5 μM, 1 hour) . **(H)** Quantification of Alexa Fluor 488-transferrin (1 μg/mL) and Alexa Fluor 488-albumin (1 μg/mL) uptake by LysM Cre^{+}/*Nf1*$^{fox/flox}$ macrophages to investigate the role of *NF1* in clathrin- and caveolin-mediated endocytosis, respectively ($n = 3$). Data represent the mean ± SEM. $^{*}p < 0.05$ vs. control, $^{\#}p < 0.05$ vs. Cre^{+} *Nf1*$^{fox/flox}$ + vehicle. NS: not significant.

receptor-mediated uptake of Alexa Fluor 488-transferrin (1 μg/mL) and Alexa Fluor 488-albumin (1 μg/mL) in LysM Cre^{+} *Nf1*$^{f/f}$ macrophages to investigate the role of neurofibromin in clathrin- and caveolin-mediated endocytosis, respectively. Our results demonstrated that loss of *Nf1* in macrophages does not stimulate clathrin- and caveolin-mediated endocytosis (Fig. 1H). Taken together, these results suggest that loss of *Nf1* stimulates macropinocytosis, but not receptor-mediated endocytosis, in macrophages.

3.2. RAS signaling is required for macropinocytosis stimulation in neurofibromin-deficient macrophages

Neurofibromin functions as a GTPase-activating protein (GAP) that negatively regulates RAS activity by accelerating the hydrolysis of Ras-bound GTP [29]. As a consequence, *Nf1*-mutant cells maintain high levels of active Ras-GTP and facilitate downstream activation of RAS kinases, including MEK/ERK and phosphatidylinositol-3-kinase (PI3K)/AKT [30–32]. As activating Ras mutations have been shown to promote macropinocytosis in cancer cells and *Dictyostelium* [13,19], we next examined whether Ras mediates macropinocytosis in *Nf1*-mutant macrophages. Western blot analysis indicated increased activity of ERK (pTyr 204) and AKT (pSer 473) in LysM Cre^{+}/*Nf1*$^{flox/flox}$ macrophages compared with Cre^{-} controls, consistent with increased Ras activity in *Nf1* null macrophages (Fig. 2A and B). Similar to our observations in *Nf1* mutant macrophages, bone marrow-derived macrophages from H-Ras^{G12V} (constitutively active mutant) mice internalized FITC-dextran at a higher rate compared to H-Ras null (H-Ras$^{-/-}$) and wild type H-Ras$^{+/+}$ macrophages (Fig. 2C). Preincubation of H-Ras^{G12V} BMDM with EIPA inhibited FITC-dextran internalization, confirming the role of RAS signaling in macropinocytosis stimulation (Fig. 2C). Downstream, Ras signaling is known to activate the p110 catalytic subunit of PI3K, a regulatory enzyme required for the conversion of PtdIns(4,5)P_2 to PtdIns(3,4,5)P_3 in the plasma membrane [33]. As macropinosomes originate from plasma membrane regions enriched in PtdIns(3,4,5)P_3 [16], we next examined whether pharmacological inhibition of PI3K inhibits macropinocytosis in *Nf1*-deficient macrophages. As shown in Fig. 2D, the pan-PI3K inhibitor LY294002 (10 μM, 30 min) completely abolished FITC-dextran accumulation in *Nf1* null macrophages. Finally, preincubation of LysM Cre^{+}/*Nf1*$^{flox/flox}$ macrophages with lonafarnib (10 μM, 30 min), a farnesyl transferase inhibitor (FTI) that inhibits posttranslational modification and activation of H-Ras [34], significantly attenuated macropinocytosis in *Nf1* knockout macrophages (Fig. 2E). Taken together, these data suggest that loss of *Nf1* stimulates macrophage macropinocytosis via Ras-mediated PI3K signaling.

3.3. Loss of Nf1 stimulates macropinocytosis via p47^{phox}-mediated Nox2 activation

PtdIns(3,4)P_2 and PtdIns(3)P bind to the Phox homology (PH) domains of Nox2 organizer subunits p47^{phox} and p40^{phox}, respectively, and

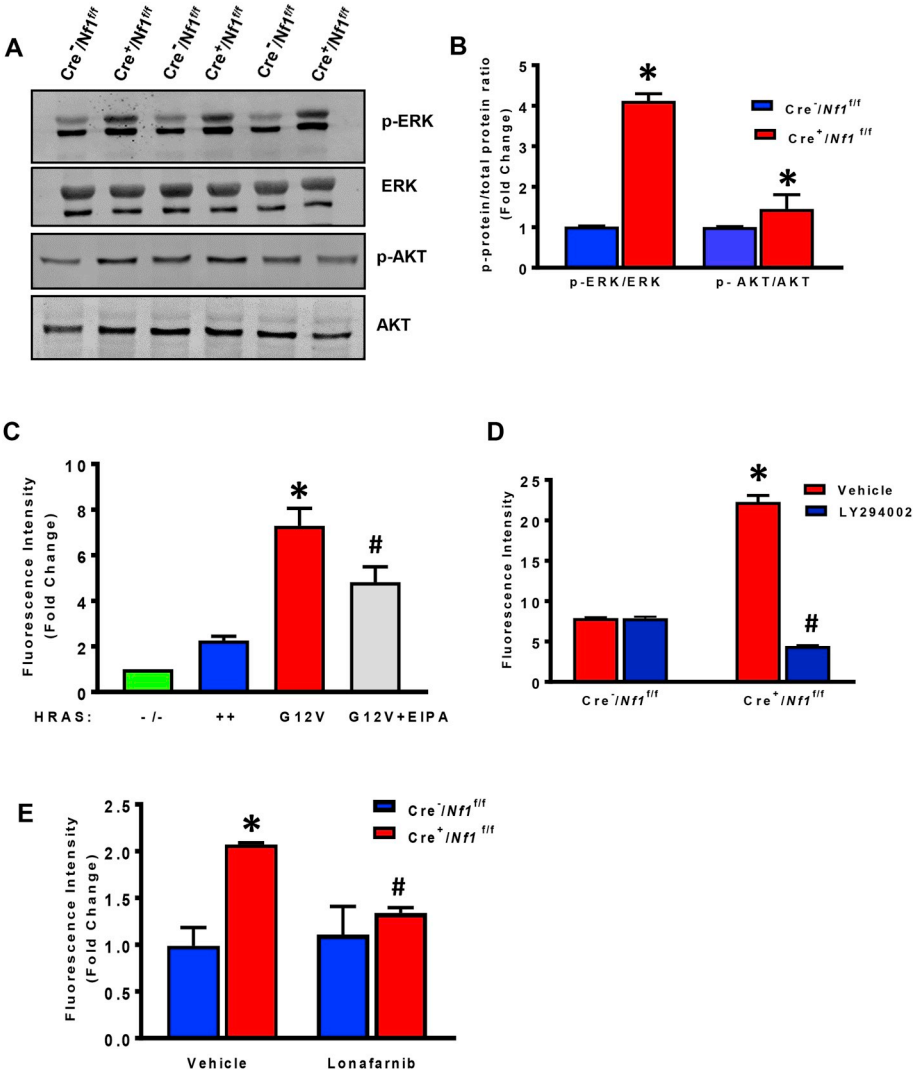

Fig. 2. RAS signaling stimulates macropinocytosis in *NF1*-deficient macrophages. **(A&B)** Bone marrow-derived macrophages from Cre^{-} and Cre^{+}/*Nf1*$^{flox/flox}$ mice were lysed and subjected to Western blot analysis using phospho- or total ERK and AKT antibodies. Representative Western blot images are shown. Bar graphs represent averaged optical-density data expressed as a ratio of phosphorylated to total proteins ($n = 3$). **(C)** Quantification of internalized FITC-dextran by BMDM from H-Ras knockout (H-Ras$^{-/-}$), wild type H-Ras$^{+/+}$ and H-Ras^{G12V} mice (+/− EIPA treatment, 10 μM, 30 min). $n = 3$, $^{*}p < 0.05$ vs. wild type, $^{\#}p < 0.05$ vs. G12V. **(D)** Cells were treated with vehicle or preincubated with the pan-PI3K inhibitor LY294002 (10 μM, 30 min) followed by FITC-dextran treatment for 16 h. Fluorescence was determined by FACS analysis ($n = 3$). **(E)** LysM Cre^{-}/*Nf1*$^{flox/flox}$ and LysM Cre^{+}/*Nf1*$^{flox/flox}$ BMDM were pretreated with lonafarnib (10 μM, 30 min) and FITC internalization was quantified by FACS ($n = 3$). Data represent the mean ± SEM. $^{*}p < 0.05$ vs. Cre^{-}/*Nf1*$^{flox/flox}$, $^{\#}p < 0.05$ vs. Cre^{+}/*Nf1*$^{flox/flox}$ + vehicle.

anchor them to the plasma membrane [35]. PtdIns(3,4,5)P_3 activates protein kinase C (PKC) [36], which in turn, phosphorylates and facilitates p47^{phox} binding to p22^{phox} leading to Nox2 assembly and $O_2^{\bullet-}$ generation [37]. However, no prior studies have investigated whether loss of *NF1* stimulates Nox2 activation in phagocytes (or any other cell types) or whether Nox2/$O_2^{\bullet-}$ mediates macropinocytosis in

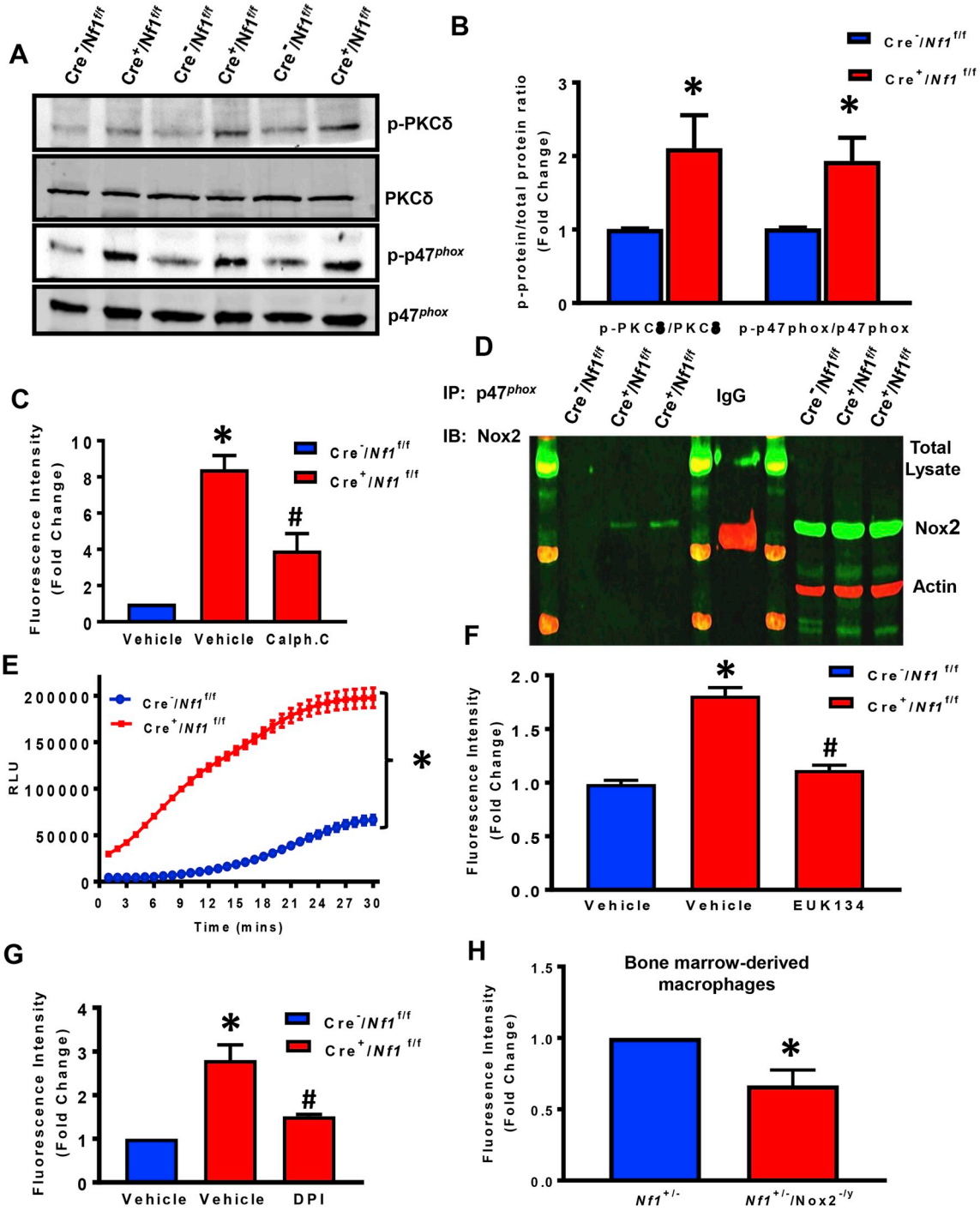

Fig. 3. P47^{phox}-mediated Nox2 activation is essential for macropinocytosis stimulation in *NF1*-deficient macrophages. **(A & B)** Western blot data indicate phosphorylation of PKCδ (pTyr 311) and p47^{phox} (pSer 345) in LysM Cre$^+$/*Nf1*$^{flox/flox}$ BMDM compared to LysM Cre$^-$/*Nf1*$^{flox/flox}$ controls ($n = 3$). The phosphorylation of PKCδ and p47^{phox} was normalized to the corresponding total protein. **(C)** Bar diagram represents FITC-dextran accumulation in LysM Cre$^+$/*Nf1*$^{flox/flox}$ macrophages pretreated with vehicle or calphostin C (1 μM, 30 min). The data were collected from three independent experiments. **(D)** Immunoprecipitation of cell lysates from Cre$^-$/*Nf1*$^{f/f}$ and Cre$^+$/*Nf1*$^{f/f}$ BMDM with an anti-p47^{phox} antibody followed by immunoblotting with an anti-Nox2 monoclonal antibody. Total Nox2 levels were evaluated in cell lysates prior to immunoprecipitation (right panel). β-actin is used as a loading control. Rabbit IgG was used as an isotype control. **(E)** ROS generation measured by L-012 chemiluminescence, $n = 3$. **(F)** DCFH fluorescence measured in LysM Cre$^+$/*Nf1*$^{flox/flox}$ BMDM ± EUK134 by flow cytometry analysis, $n = 3$. **(G)** Cells were treated with vehicle or preincubated with diphenyleneiodonium (DPI, 5 μM, 30 min), then treated with FITC-dextran, and fluorescence analyzed by FACS ($n = 3$). **(H)** Quantification of FITC–dextran accumulation by bone marrow derived macrophages from *Nf1*$^{+/-}$ controls (blue) compared with *Nf1*$^{+/-}$/Nox2$^{-/y}$ cells (red) ($n = 3$). Data represent the mean ± SEM. $^*p < 0.05$ vs. Cre$^-$/*Nf1*$^{f/f}$ and $^{\#}p < 0.05$ vs. Cre$^+$/*Nf1*$^{f/f}$ + vehicle.

neurofibromin-deficient cells. Western blot data support this hypothesis as indicated by increased expression of the active form of PKCδ (pTyr 311) and p47^{phox} (pSer 345) and stable expression of total proteins in LysM Cre^{+}/*Nf1*$^{flox/flox}$ macrophages when compared with wild type controls (Fig. 3A and B). Previous reports showed that Ras-dependent phosphorylation of p47^{phox} is mediated by PKCδ in Ras^{G12V} over-expressing fibroblasts compared with wild type Ras-transduced controls, demonstrating the role of PKC activation downstream of Ras signaling [38]. Supporting this relationship, we observed that pre-incubation of LysM Cre^{+}/*Nf1*$^{flox/flox}$ macrophages with calphostin C, an

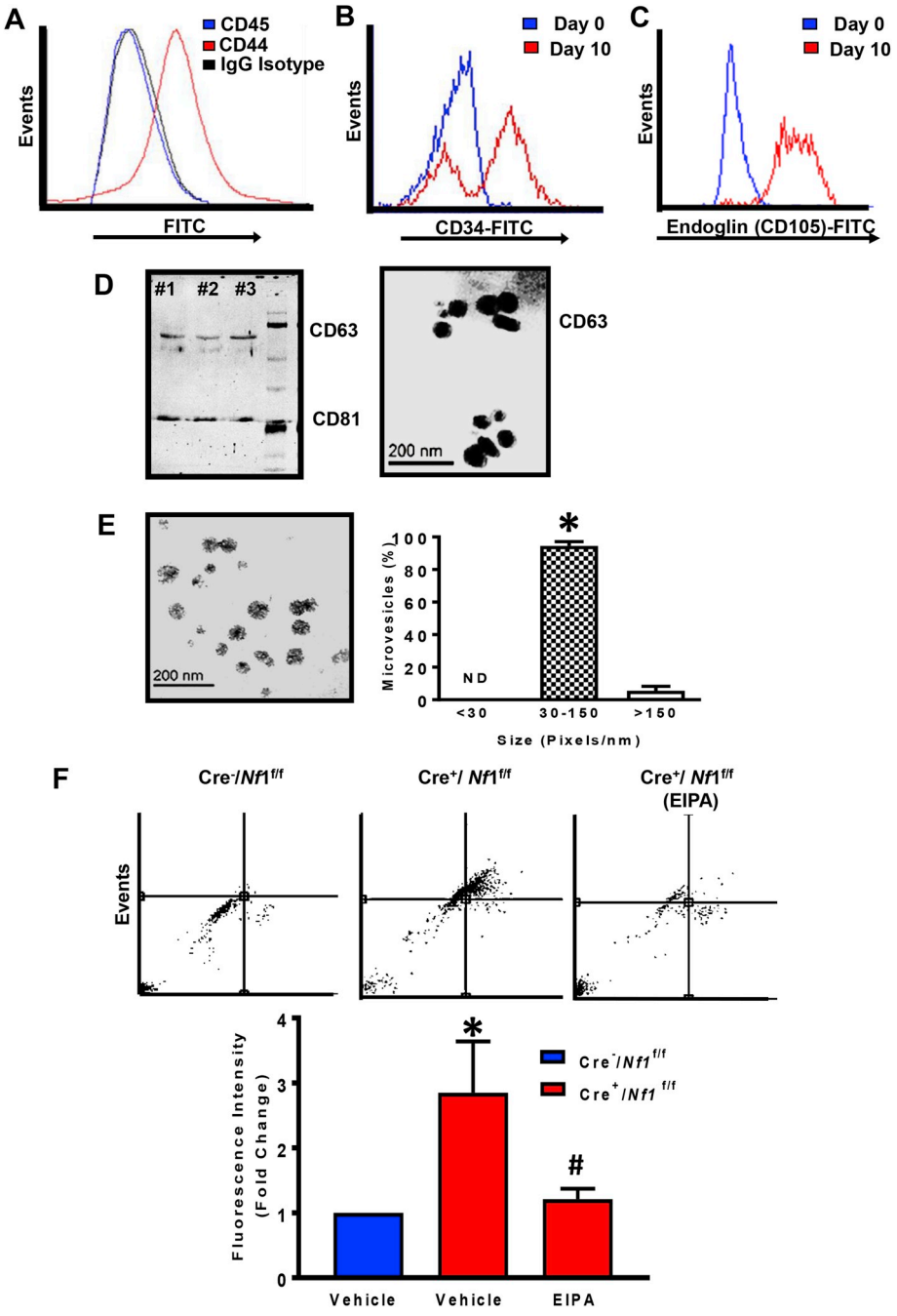

Fig. 4. Macropinocytosis facilitates exosomes uptake by *Nf1*-deficient macrophages *in vitro* and *in vivo*. **(A)** Representative FACS histograms of bone marrow-derived mesenchymal stem cells (MSC) expressing CD44 but not CD45. Mouse IgG has been used as an isotype control antibody. **(B&C)** Flow cytometry analysis at day 0 and day 10 of differentiation for endoglin (CD105) and CD34 expression. **(D)** Immunoblotting analysis and immunogold labeling confirm expression of exosomal marker molecules CD63 and CD81. **(E)** The morphology of exosomes was visualized by transmission electron microscopy (TEM). Scale bar: 200 nm. The bar diagram represents size-based separation of endothelial cell-derived microvesicles ($n = 3$). **(F)** Cre^{-}/*Nf1*$^{flox/flox}$ and Cre^{+}/*Nf1*$^{flox/flox}$ macrophages were incubated with fluorescently labeled (PKH67) endothelial cell-derived exosomes (10 μg/mL, 24 h) in the absence and presence of macropinocytosis inhibitor EIPA. *Upper panel* shows a representative dot blot of FITC fluorescence. *Lower panel* indicates quantification of fluorescence intensity fold change between *NF1*-deficient vs. wild type macrophages ($n = 3$). **(G)** Confocal imaging demonstrating incorporation of fluorescently-labeled (PKH67, green) exosomes by wild type and *NF1*-deficient macrophages in the absence and presence of EIPA or EUK134. Hoechst (blue) has been used for nuclear staining ($n = 3$). **(H)** Bar graph representing fluorescence intensity fold change in Cre^{-}/*Nf1*$^{flox/flox}$ and Cre^{+}/*Nf1*$^{flox/flox}$ peritoneal macrophages following intraperitoneal injection of PKH67-labeled endothelial cell exosomes. Data represent the mean ± SEM. $^{*}p < 0.05$ vs. Cre^{-}/*Nf1*$^{flox/flox}$ + vehicle, $^{\#}p < 0.05$ vs. Cre^{+}/*Nf1*$^{flox/flox}$ + vehicle.

inhibitor of conventional and novel PKC isoforms, significantly attenuated FITC-dextran accumulation (Fig. 3C).

Next, we sought to examine the interactions between $p47^{phox}$ and Nox2 in *Nf1* null and wild type BMDM. Immunoprecipitation of $p47^{phox}$ in macrophage lysates confirmed a direct association between $p47^{phox}$ with Nox2 in neurofibromin-deficient macrophages (Fig. 3D). Next, we measured ROS generation using the luminol-based chemiluminescent probe L-012 and cell-permeant fluorescent reagent DCFH. As demonstrated in Fig. 3E and F, *Nf1* null macrophages displayed significantly increased ROS generation compared with wild type macrophages. L-012 chemiluminescence expressed as area under the curve (AUC) is shown in Supplementary Fig. S3. Further, we defined the functional role of ROS in macropinocytosis stimulation in neurofibromin-deficient macrophages using the cell permeant SOD/catalase mimetic EUK134. As shown in Fig. 3F, pretreatment of neurofibromin-deficient macrophages with EUK134 abolished FITC-dextran internalization. Because Nox2 has been previously suggested to participate in macropinocytosis [39], we postulated that enhanced macropinocytosis in *Nf1* null

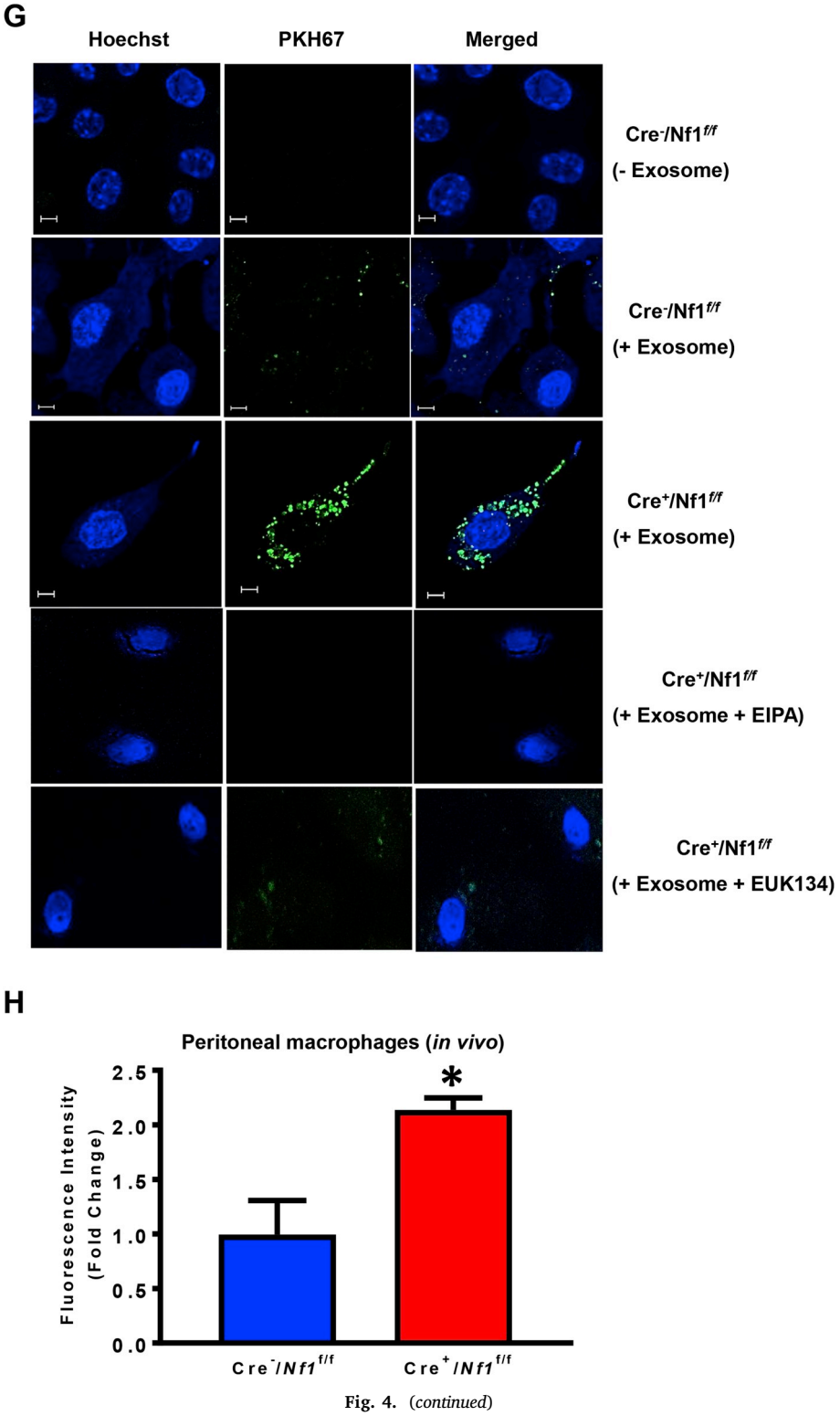

Fig. 4. (*continued*)

macrophages occurs via Nox2 activation. Diphenyleneiodonium (DPI), a broad-profile flavoprotein inhibitor of Nox isoforms, significantly attenuated FITC-dextran uptake in *Nf1* null macrophages (Fig. 3G). Moreover, we generated *Nf1*$^{+/-}$/Nox2$^{y/-}$ mice and demonstrated that absence of Nox2 in *Nf1*-deficient macrophages inhibits FITC-dextran internalization (Fig. 3H). Consistent with these results, gene-silencing Nox2 in *Nf1*-deficient macrophages using siRNA inhibited FITC-dextran internalization (Supplementary Fig. S4). Effective silencing of Nox2 is shown in Supplementary Fig. S4. In summary, these results suggest that loss of neurofibromin stimulates macrophage macropinocytosis by PKC-mediated p47^{phox} phosphorylation and Nox2-derived ROS generation.

3.4. Macropinocytosis stimulation in neurofibromin-deficient macrophages potentiates cellular uptake of exosomes in vitro and in vivo

Multivesicular bodies formed in endothelial cells can fuse with the basolateral plasma membrane and release exosomes into the sub-endothelial layer, an area into which monocytes transmigrate and become macrophages during inflammation. Neurofibromin-deficient macrophages accumulate near the internal elastic lamina and medial layer in neurofibromatosis and functionally contribute to the pathogenesis of NF1 vasculopathy, particularly in murine models of aortic aneurysm [8,9]. These findings prompted us to examine whether exosomes derived from AngII-treated endothelial cells are internalized by LysM Cre^{+}/*Nf1*$^{flox/flox}$ macrophages via macropinocytosis. In these experiments, we used AngII to stimulate wild type endothelial cell release of exosomes because *a*) renal artery stenosis is associated with activation of the renin-angiotensin-aldosterone (RAAS) system in NF1 patients [40] and *b*) AngII-infusion promotes aneurysm formation in animal models of neurofibromatosis [8]. Bone marrow-derived mesenchymal stem cells (MSC) (CD45^{-}/CD44^{+}; Fig. 4A) were isolated from C57Bl/6 wild type mice and differentiated into endothelial-like

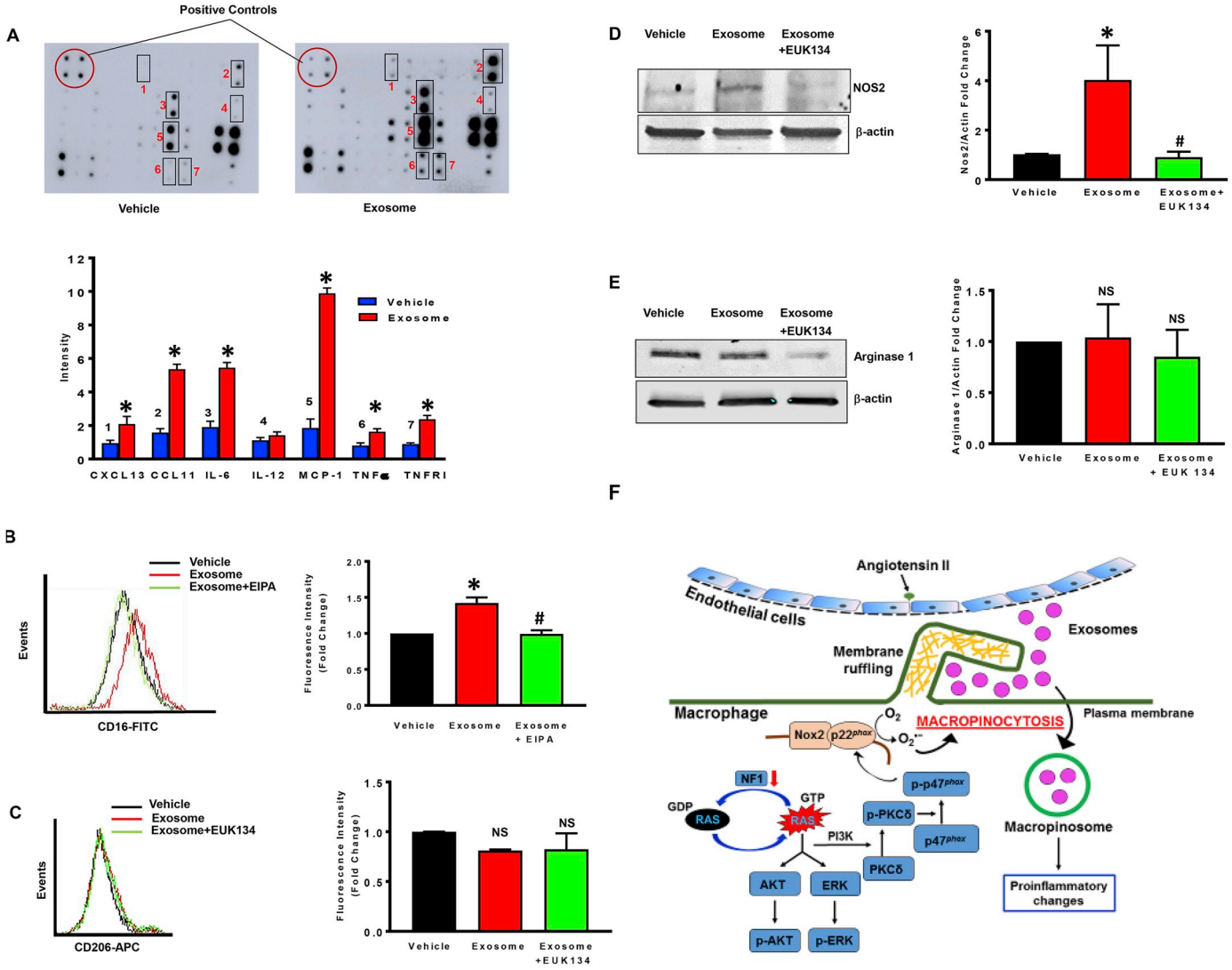

Fig. 5. *NF1*-deficient macrophages secrete pro-inflammatory cytokines following internalization of endothelial cell-derived exosomes.
(A) *NF1* null macrophages were incubated with vehicle or AngII-EC exosomes (50 μg/mL, 24 h) and cytokine secretion into the media was quantified using a membrane-based sandwich immunoassay ($n = 3$). The original representative membranes are shown in the *upper panel*. In the *lower panel*, averaged relative intensity of pixels reflecting levels of expression for selected proteins are shown. **(B)** *NF1* null macrophages were treated with vehicle or AngII-EC exosomes with or without EIPA. CD16 expression was analyzed by FACS ($n = 3$). **(C)** Macrophages lacking *NF1* were treated with vehicle or AngII-EC exosomes with or without EUK134. CD206 expression was analyzed by FACS ($n = 3$). **(D)** Western blot of NOS2 in *NF1*-deficient macrophages treated with AngII-EC exosomes (50 μg/mL) or PBS for 24 h with or without EUK134 ($n = 3$). Data represent the mean ± SEM. $^{*}p < 0.05$ vs. vehicle, $^{\#}p < 0.05$ vs. exosome-treated. **(E)** Western blot of arginase-1 in *NF1*-deficient macrophages treated with AngII-EC exosomes (50 μg/mL) or PBS for 24 h with or without EUK134 ($n = 3$). Data represent the mean ± SEM. $^{*}p < 0.05$ vs. vehicle, $^{\#}p < 0.05$ vs. exosome-treated. NS: not significant. **(F)** Schematic summary of findings: *NF1* loss of function stimulates macropinocytosis by activation of the Ras/PKCδ/p47^{phox}/Nox2 pathway, which in turn facilitates exosome uptake and proinflammatory changes in macrophages.

cells in the presence of 2% FCS and 50 ng/mL VEGF for 10 days [41]. Flow cytometry analysis demonstrated increased expression of endothelial markers, CD34 and endoglin (CD105), on the surface of differentiated MSC, while Western blot analysis and immuno-gold labeling confirmed expression of exosomal marker molecules, CD63 and CD81, in the exosome preparations (Fig. 4B–D). Transmission electron microscopy (TEM) was performed to visualize the morphology of secreted microvesicles and investigate whether they fall into the expected size range of exosomes (30–150 nm). Image J analysis demonstrated that majority (~90%) of endothelial cell-derived microvesicles were exosomes (Fig. 4E). Next, $Cre^{-}/Nf1^{f/f}$ and $Cre^{+}/Nf1^{f/f}$ macrophages were incubated with fluorescently labeled (PKH67) exosomes (10 μg/mL, 24 h) derived from AngII-treated endothelial cells in the absence and presence of macropinocytosis inhibitor EIPA. FACS analysis and confocal imaging demonstrated increased internalization of fluorescently labeled endothelial cell-derived exosomes by neurofibromin-deficient macrophages when compared with wild type controls (Fig. 4F and G). Preincubation of neurofibromin-deficient macrophages with EIPA abolished exosome internalization, suggesting a role for macropinocytosis in exosome uptake (Fig. 4F and G).

With these findings in mind, we postulated that loss of *Nf1* in macrophages stimulates exosome internalization *in vivo*. To test this, we used a validated *in vivo* model of macrophage macropinocytosis with some modifications [20,39,42]. Briefly, $Cre^{-}/Nf1^{f/f}$ and $Cre^{+}/Nf1^{f/f}$ mice received 2% thioglycollate via intraperitoneal (ip.) injection to elicit macrophages to the peritoneum. After 3 days, $Cre^{-}/Nf1^{f/f}$ and $Cre^{+}/Nf1^{f/f}$ mice were injected ip. with fluorescently labeled exosomes (15 mg protein in 50 μl sterile saline). Macrophages were isolated using peritoneal lavage 24 h later, fixed and assessed for exosome accumulation using FACS. As shown in Fig. 4H, loss of *Nf1* function enhanced exosome internalization in peritoneal macrophages by approximately 2-fold compared to Cre^{-} controls. Taken together, these results suggest that loss of *Nf1* in macrophages stimulates macropinocytotic internalization of endothelial cell-derived exosomes *in vitro* and *in vivo*.

3.5. Internalization of endothelial cell-derived exosomes promotes polarization of neurofibromin-deficient macrophages toward a proinflammatory phenotype

Macrophages display remarkable plasticity and can change their phenotype and function in response to environmental cues [43]. Next, we tested the hypothesis that internalization of AngII-treated endothelial cell-derived (AngII-EC) exosomes by neurofibromin-deficient macrophages promotes their phenotypic and functional changes relevant to the pathogenesis of NF1 vasculopathy. *Nf1* null macrophages were incubated with vehicle (no exosomes) or AngII-EC exosomes (50 μg/mL; 24 h) and cytokine secretion into the media was determined using membrane-based sandwich immunoassay according to the manufacturer's instructions (Raybiotech, USA). Quantification of the relative signal intensity indicated stimulated secretion of CXCL13, CCL11, IL-6, MCP-1, TNF-α and TNF RI in AngII-EC exosome-treated NF1-deficient macrophages compared with control cells (Fig. 5A). Secretion of IL-12 into the media was not different between groups, while IL-10, IFN-gamma and CXCL9 were undetectable.

The macrophage phenotype spectrum is characterized, at the extremes, by classically activated M1 and alternatively activated M2 macrophages [44]. Interestingly, the secreted proinflammatory cytokines by AngII-EC exosome-treated *Nf1* null macrophages in Fig. 5A experiments have been previously characterized as signature markers for M1 polarization [45,46]. To examine the M1 and M2 polarization status of *Nf1* null macrophages treated with AngII-EC exosomes, we quantified plasma membrane expression of classical M1 [CD16 and NOS2 [46]] and M2 [CD206 and Arg-1 [47]] markers using FACS analysis and Western blotting. Incubation of neurofibromin-deficient macrophages with AngII-EC exosomes stimulated CD16, but not CD206, expression when compared with vehicle treatment (Fig. 5B and C). Importantly, incubation of *Nf1* null macrophages with exosomes derived from vehicle-treated endothelial cells (Vehicle-EC) did not stimulate CD16 expression (Fig. S5). Preincubation of *Nf1* null macrophages with the macropinocytosis inhibitor EIPA (10 μM, 30 min) and the antioxidant EUK134 (10 μM, 1 h) diminished AngII-EC exosome-induced increase in CD16 expression, suggesting that macropinocytosis of AngII-EC exosomes stimulates M1 polarization (Fig. 5B, S6). Western blot experiments demonstrated that treatment of neurofibromin-deficient macrophages with AngII-EC exosomes stimulates NOS2 protein expression when compared with vehicle treatment (Fig. 5D). The levels of Arg-1 remained unchanged in exosome-treated vs. control cells (Fig. 5E). Finally, we found that pretreatment of *Nf1* null macrophages with EUK134 decreased AngII-EC exosome-induced NOS2 expression. Taken together, these results suggest that internalization of exosomes derived from AngII-treated endothelial cells promotes polarization of neurofibromin-deficient macrophages toward a proinflammatory M1 phenotype.

4. Discussion

Individuals with neurofibromatosis type 1 often develop cardiovascular diseases, ranging from developmental defects in the heart to acquired manifestations later in life including arterial stenosis, arteriovenous malformations, aneurysms and systemic hypertension. These cardiovascular diseases contribute to the excess morbidity and mortality observed in children and young adults with NF1 [7]. Despite these observations, targeted pharmacological strategies for NF1-associated vascular disorders do not exist, which is largely due to a limited understanding of disease pathogenesis. Human and animal data suggest that monocytes and macrophages play key roles in the pathogenesis of NF1-associated vascular diseases [8,9,11]. The specific mechanisms, however, by which monocytes/macrophages contribute to the vascular complications of NF1 remain unknown.

Neurofibromin is a negative regulator of RAS and mutations in *NF1* diminish neurofibromin expression and/or function, leading to increased RAS activity. Neurofibromin functions as a RAS GAP for multiple members of the RAS family, therefore long-term pan-RAS inhibition would likely be needed for the treatment of NF1-associated pathologies [48]. Such pharmacological approaches are unrealistic owing to the highly conserved nature of RAS proteins and unwanted effects on their downstream targets in normal cell growth and physiology [49]. Interestingly, previous studies demonstrated that Ras activation in cancer cells stimulates macropinocytosis *in vitro* [50] and pharmacological inhibition of macropinocytosis attenuates tumor growth *in vivo* [13]. As patients with NF1 are prone to develop various non-nervous and nervous system tumors [51], we postulated that activation of RAS in neurofibromin-deficient cells stimulates macropinocytosis. Relevant to this hypothesis, a recent study demonstrated that axenic *Dictyostelium* internalize dissolved nutrients via neurofibromin-regulated macropinocytosis [19]. To our knowledge, no prior studies investigated whether *a*) neurofibromin regulates macropinocytosis in mammalian cells, *b*) the potential signaling pathways by which loss of *NF1* stimulates macropinocytosis and *c*) the possible macrophage-related mechanisms leading to the vascular phenotypes observed in NF1. In the present study, we employed macrophages isolated from either $Nf1^{+/-}$ or Lysm $Cre^{-}/Cre^{+}Nf1^{flox/flox}$ mice to investigate macropinocytosis in neurofibromin-deficient cells. Flow cytometry analysis demonstrated that $LysmCre^{+}/Nf1^{flox/flox}$ macrophages internalize FITC-dextran at a higher rate compared with $LysmCre^{-}$ $Nf1^{f/f}$ controls. Similarly, heterozygous inactivation of *NF1* ($Nf1^{+/-}$) stimulated FITC-dextran uptake in macrophages compared with wild type macrophages. Quantification of membrane ruffles revealed significantly increased ruffling on the surface of $LysmCre^{+}/Nf1^{flox/flox}$ macrophages compared with Cre^{-} controls. M-CSF (used for BMDM differentiation in these experiments) is able to stimulate macrophage macropinocytosis [22]. It is important to note that all FITC-dextran

internalization experiments were performed after 24 h of incubation in MCSF-free media. Increased internalization of FITC-dextran was also confirmed in neurofibromin-deficient peritoneal macrophages that were not treated with exogenous M-CSF.

Next, we examined whether neurofibromin deficiency stimulates internalization of FITC-dextran via macropinocytosis by contrasting its potential contribution with that of other endocytic processes. Macropinocytosis is characterized by its sensitivity to actin perturbants [28] and inhibitors of PI3K [21]. We observed that both cytochalasin D and LY294002 completely inhibited FITC-dextran accumulation in neurofibromin-deficient macrophages. An additional criterion was applied to identify macropinocytosis; namely, its susceptibility to inhibition by the selective NHE blocker EIPA, which is considered to be the first choice inhibitor for pharmacological blockade of macropinocytosis [13,52]. Indeed, preincubation of macrophages with EIPA abolished FITC-dextran uptake in neurofibromin-deficient macrophages. In addition, imipramine, a newly identified inhibitor of macropinocytosis [26], inhibited FITC-dextran internalization by *Nf1* null macrophages. We also quantified receptor-mediated transferrin and albumin uptake in LysmCre^{+}/*Nf1*$^{flox/flox}$ macrophages to investigate whether loss of *Nf1* stimulates clathrin- and caveolin-mediated endocytosis, respectively. Our results demonstrated that neurofibromin-deficient macrophages did not internalize more transferrin or albumin when compared with wild type controls. To our knowledge, these data are the first to demonstrate that deletion of *Nf1* in macrophages stimulates macropinocytosis.

Members of the Ras superfamily of small guanosine triphosphatases (GTPases), Ras, Rac, Cdc42, Arf 6 and Rab5, have been reported to promote macropinocytic activity [53]. Ras activation leads to downstream stimulation of MEK/ERK and PI3K/AKT pathways and both pathways are activated in LysmCre^{+}/*Nf1*$^{flox/flox}$ macrophages [54]. To confirm the role of active Ras in macropinocytosis stimulation, we incubated BMDM from H-Ras$^{-/-}$, H-Ras$^{+/+}$, and H-Ras^{G12V} mice with FITC-dextran and quantified uptake using FACS. H-Ras^{G12V} macrophages internalized FITC-dextran at a higher rate compared with H-Ras$^{-/-}$ and H-Ras$^{+/+}$ macrophages, and the internalization was sensitive to pharmacological inhibition of macropinocytosis by EIPA. Consistent with these results, lonafarnib, a farnesyl transferase inhibitor of H-Ras, decreased FITC-dextran internalization by neurofibromin-deficient macrophages. Previous studies reported that 3-phosphorylated phosphoinositides play a critical role in the initiation and completion of macropinocytosis [55]. Importantly, Ras activates the p110 catalytic subunit of PI3K, a regulatory enzyme required for the phosphorylation of phosphatidylinositol (PtdIns) to PtdIns(3)P, PtdIns(3,4)P_2 and PtdIns (3,4,5)P_3. Consistent with the role of 3-phosphorylated phosphoinositides, we demonstrated that preincubation of *Nf1*-null macrophages with the PI3K inhibitor LY294002 completely abolishes FITC-dextran internalization. Taken together, these results suggest that PI3K activation downstream of Ras and subsequent generation of 3-phosphorylated PtdIns mediate macropinocytosis in neurofibromin-deficient macrophages.

NADPH oxidase 2 (Nox2) in "*professional*" phagocytic cells is a multicomponent enzyme that consists of the membrane-bound Nox2 and p22^{phox} and several cytosolic adaptor proteins [56]. Reduction of molecular oxygen to $O_2^{\bullet -}$ by Nox2-mediated electron transport requires translocation of the cytosolic subunits, p47^{phox}, p67^{phox}, p40^{phox} and Rac1, to Nox2 and p22^{phox}. PKC-mediated phosphorylation of serine residues within the autoinhibitory region (AIR) of p47^{phox} exposes the SH3 domain allowing its interaction with p22^{phox} and revealing its binding sites for interaction with plasma membrane PtdIns (3,4)P_2 [37]. Interestingly, PtdIns(3)P has been shown to bind to the PH domain of p40^{phox}, thus playing a role in Nox2 assembly also [35]. Based on these results, we examined whether Nox2 mediates macropinocytosis stimulation in neurofibromin-deficient macrophages. Western blot data indicated activating phosphorylation of PKCδ [a major PKC isoform in macrophages [14]] and p47^{phox} in LysmCre^{+}/*Nf1*$^{flox/flox}$ macrophages when compared with controls. Immunoprecipitation of p47^{phox} followed by immunoblotting with an anti-Nox2 antibody, indicated association of Nox2 with p47^{phox} in *Nf1* null, but not in wild type, macrophages. Functional assembly of Nox2 in neurofibromin-deficient cells was confirmed by chemiluminescent and fluorescent ROS detection techniques. Calphostin c, DPI and EUK134 blocked FITC-dextran internalization in neurofibromin-deficient macrophages demonstrating that PKC and ROS derived from a DPI-inhibitable enzymatic source are required for stimulation of macropinocytosis. Next, we generated *Nf1*$^{+/-}$/Nox2$^{y/-}$ mice to investigate whether loss of Nox2 attenuates macropinocytosis stimulation in NF1-deficient macrophages. Our results demonstrated that exosome internalization is significantly attenuated in Nox2 knockout *Nf1*$^{+/-}$ macrophages compared with Nox2$^{y/+}$ controls. Consistent with these results, a previous study showed that deletion of Nox2 in myeloid cells inhibits neointima formation in *Nf1*$^{+/-}$ mice [57]. A previous study reported that loss of NF1 signaling in *Dictyostelium* stimulates Ras activity and actin polymerization, leading to macropinocytosis [19]. Relevant to this, previous studies from our laboratory demonstrated that increased Nox2 activity via activation of slingshot phosphatase-1 (SSH1) stimulates cofilin dephosphorylation, leading to membrane ruffling and macropinocytosis [17,39]. With regard to the downstream redox signaling mechanisms stimulating actin remodeling and macropinocytosis in NF1-deficient macrophages, we speculate that PKCδ/Nox2-mediated activation of SSH1 induces activation of cofilin, leading to actin remodeling and macropinocytosis [14,17]. In that respect, we expect future studies to investigate the role of SSH1 and cofilin (or other actin binding proteins) in macropinocytosis stimulation in *NF1*-deficient macrophages.

Vascular cell-derived exosomes have recently been regarded as important intercellular signaling messengers mediating vascular remodeling and cardiovascular disease [58]. Endothelial cells can release exosomes into the circulation and the subendothelial layer of arterial wall. Previous studies have demonstrated that neurofibromin-deficient macrophages accumulate near the internal elastic lamina and medial layer in neurofibromatosis and functionally contribute to the pathogenesis of NF1-related aortic aneurysm formation and arterial stenosis [8,11]. Therefore, we tested the hypothesis that exosomes derived from AngII-treated endothelial cells are internalized by LysM Cre^{+}/*Nf1*$^{flox/flox}$ macrophages via macropinocytosis. We elected to stimulate endothelial cells with AngII prior to exosome collection because AngII appears to contribute to the pathogenesis of both human and murine NF1 vasculopathy [8,40]. Flow cytometry analysis and confocal imaging showed increased internalization of fluorescently labeled endothelial cell-derived exosomes by neurofibromin-deficient macrophages compared with wild type macrophages. EIPA inhibited internalization of exosomes by neurofibromin-deficient macrophages, suggesting that macropinocytosis is the primary uptake mechanism. Shifting to an *in vivo* approach, we determined the role of neurofibromin in exosome internalization by residential macrophages in the peritoneal cavity. Our results indicated that peritoneal macrophages in LysM Cre^{+}/*Nf1*$^{flox/flox}$ mice internalized significantly more endothelial cell-derived exosomes when compared with wild type macrophages from Cre^{-} mice. As a consequence of exosome internalization neurofibromin-deficient macrophages expressed higher levels of M1 polarization markers and secreted proinflammatory cytokines. Given previously published findings demonstrating the role of exosomes in the pathomechanisms of vascular disorders [58], we speculate that endothelial cell exosome-mediated paracrine cell communication driven by stimulated macrophage macropinocytosis may contribute to the inflammatory vascular phenotype observed in neurofibromatosis.

A limitation of the present study is that we did not directly investigate the role of macrophage macropinocytosis in the pathogenesis of *Nf1*$^{+/-}$-driven vascular disorders. Moreover, a more comprehensive study utilizing miRNA and protein arrays is needed to identify the specific endothelial cell-derived mediators that contribute to the proinflammatory changes in macrophages. Furthermore, our study

raises the possibility that lack of neurofibromin stimulates macropinocytosis in other cell types (e.g.: Schwann cells), leading to their increased proliferation and NF1-associated malignant disorders. These research areas are currently a focus of intense interest in our laboratory and outside of the scope of the present study.

In conclusion, our findings identify a previously unknown mechanism of solute internalization stimulated via a neurofibromin/Ras/PKCδ/$p47^{phox}$/Nox2/macropinocytosis pathway that may have important implications for the vascular and malignant complications of NF1. The present study highlights the importance of macropinocytosis in intercellular communication and regulation of phenotypic and functional changes in recipient cells. Taken together, these findings may contribute to a better understanding of how neurofibromin deficiency leads to NF1-associated vascular disorders and identify new therapeutic targets for the vascular complications of this human disease.

Acknowledgments

The authors would like to thank Jeanene Pihkala, Libby Perry and Brendan Marshall (Augusta University) for their help with the FACS analysis, SEM sample preparation and TEM sample imaging, respectively.

Appendix A. Supplementary data

Supplementary data to this article can be found online at https://doi.org/10.1016/j.redox.2019.101224.

Sources of funding

This work was supported by National Institutes of Health grants (4R00HL114648-03 and 1R01HL139562-01A1) awarded to Gabor Csanyi.

References

[1] K. DeBella, J. Szudek, J.M. Friedman, Use of the national institutes of health criteria for diagnosis of neurofibromatosis 1 in children, Pediatrics 105 (3 Pt 1) (2000) 608–614.
[2] A. Abramowicz, M. Gos, Neurofibromin in neurofibromatosis type 1 - mutations in NF1gene as a cause of disease, Dev Period Med 18 (3) (2014) 297–306.
[3] K.K. Hiatt, D.A. Ingram, Y. Zhang, G. Bollag, D.W. Clapp, Neurofibromin GTPase-activating protein-related domains restore normal growth in Nf1-/- cells, J. Biol. Chem. 276 (10) (2001) 7240–7245.
[4] B.K. Stansfield, W.K. Bessler, R. Mali, J.A. Mund, B.D. Downing, R. Kapur, et al., Ras-Mek-Erk signaling regulates Nf1 heterozygous neointima formation, Am. J. Pathol. 184 (1) (2014) 79–85.
[5] G.S. Oderich, T.M. Sullivan, T.C. Bower, P. Gloviczki, D.V. Miller, D. Babovic-Vuksanovic, et al., Vascular abnormalities in patients with neurofibromatosis syndrome type I: clinical spectrum, management, and results, J. Vasc. Surg. 46 (3) (2007) 475–484.
[6] J.M. Friedman, J. Arbiser, J.A. Epstein, D.H. Gutmann, S.J. Huot, A.E. Lin, et al., Cardiovascular disease in neurofibromatosis 1: report of the NF1 cardiovascular task force, Genet. Med. 4 (3) (2002) 105–111.
[7] S.A. Rasmussen, Q. Yang, J.M. Friedman, Mortality in neurofibromatosis 1: an analysis using U.S. death certificates, Am. J. Hum. Genet. 68 (5) (2001) 1110–1118.
[8] F. Li, B.D. Downing, L.C. Smiley, J.A. Mund, M.R. Distasi, W.K. Bessler, et al., Neurofibromin-deficient myeloid cells are critical mediators of aneurysm formation in vivo, Circulation 129 (11) (2014) 1213–1224.
[9] E.A. Lasater, F. Li, W.K. Bessler, M.L. Estes, S. Vemula, C.M. Hingtgen, et al., Genetic and cellular evidence of vascular inflammation in neurofibromin-deficient mice and humans, J. Clin. Investig. 120 (3) (2010) 859–870.
[10] P. Carmeliet, L. Moons, D. Collen, Mouse models of angiogenesis, arterial stenosis, atherosclerosis and hemostasis, Cardiovasc. Res. 39 (1) (1998) 8–33.
[11] B.K. Stansfield, W.K. Bessler, R. Mali, J.A. Mund, B. Downing, F. Li, et al., Heterozygous inactivation of the Nf1 gene in myeloid cells enhances neointima formation via a rosuvastatin-sensitive cellular pathway, Hum. Mol. Genet. 22 (5) (2013) 977–988.
[12] C.E. Prada, E. Jousma, T.A. Rizvi, J. Wu, R.S. Dunn, D.A. Mayes, et al., Neurofibroma-associated macrophages play roles in tumor growth and response to pharmacological inhibition, Acta Neuropathol. 125 (1) (2013) 159–168.
[13] C. Commisso, S.M. Davidson, R.G. Soydaner-Azeloglu, S.J. Parker, J.J. Kamphorst, S. Hackett, et al., Macropinocytosis of protein is an amino acid supply route in Ras-transformed cells, Nature 497 (7451) (2013) 633–637.
[14] B. Singla, P. Ghoshal, H. Lin, Q. Wei, Z. Dong, G. Csanyi, PKCdelta-mediated Nox2 activation promotes fluid-phase pinocytosis of antigens by immature dendritic cells, Front. Immunol. 9 (2018) 537.
[15] J.R. Chubb, A. Wilkins, G.M. Thomas, R.H. Insall, The Dictyostelium RasS protein is required for macropinocytosis, phagocytosis and the control of cell movement, J. Cell Sci. 113 (Pt 4) (2000) 709–719.
[16] O. Hoeller, P. Bolourani, J. Clark, L.R. Stephens, P.T. Hawkins, O.D. Weiner, et al., Two distinct functions for PI3-kinases in macropinocytosis, J. Cell Sci. 126 (Pt 18) (2013) 4296–4307.
[17] B. Singla, H.P. Lin, P. Ghoshal, M. Cherian-Shaw, G. Csanyi, PKCdelta stimulates macropinocytosis via activation of SSH1-cofilin pathway, Cell. Signal. 53 (2019) 111–121.
[18] I. Nakase, M. Niwa, T. Takeuchi, K. Sonomura, N. Kawabata, Y. Koike, et al., Cellular uptake of arginine-rich peptides: roles for macropinocytosis and actin rearrangement, Mol. Ther. 10 (6) (2004) 1011–1022.
[19] G. Bloomfield, D. Traynor, S.P. Sander, D.M. Veltman, J.A. Pachebat, R.R. Kay, Neurofibromin controls macropinocytosis and phagocytosis in Dictyostelium, Elife 4 (2015).
[20] G. Csanyi, D.M. Feck, P. Ghoshal, B. Singla, H. Lin, S. Nagarajan, et al., CD47 and Nox1 mediate dynamic fluid-phase macropinocytosis of native LDL, Antioxidants Redox Signal. 26 (16) (2017) 886–901.
[21] H.S. Kruth, N.L. Jones, W. Huang, B. Zhao, I. Ishii, J. Chang, et al., Macropinocytosis is the endocytic pathway that mediates macrophage foam cell formation with native low density lipoprotein, J. Biol. Chem. 280 (3) (2005) 2352–2360.
[22] B.E. Potts, M.L. Hart, L.L. Snyder, D. Boyle, D.A. Mosier, S.K. Chapes, Differentiation of C2D macrophage cells after adoptive transfer, Clin. Vaccine Immunol. 15 (2) (2008) 243–252.
[23] F. Chen, D. Pandey, A. Chadli, J.D. Catravas, T. Chen, D.J. Fulton, Hsp90 regulates NADPH oxidase activity and is necessary for superoxide but not hydrogen peroxide production, Antioxidants Redox Signal. 14 (11) (2011) 2107–2119.
[24] P. Ghoshal, A.J. Nganga, J. Moran-Giuati, A. Szafranek, T.R. Johnson, A.J. Bigelow, et al., Loss of the SMRT/NCoR2 corepressor correlates with JAG2 overexpression in multiple myeloma, Cancer Res. 69 (10) (2009) 4380–4387.
[25] R.J. Lobb, M. Becker, S.W. Wen, C.S. Wong, A.P. Wiegmans, A. Leimgruber, et al., Optimized exosome isolation protocol for cell culture supernatant and human plasma, J. Extracell. Vesicles 4 (2015) 27031.
[26] H.P. Lin, B. Singla, P. Ghoshal, J.L. Faulkner, M. Cherian-Shaw, P.M. O'Connor, et al., Identification of novel macropinocytosis inhibitors using a rational screen of Food and Drug Administration-approved drugs, Br. J. Pharmacol. 175 (18) (2018) 3640–3655.
[27] M. Koivusalo, C. Welch, H. Hayashi, C.C. Scott, M. Kim, T. Alexander, et al., Amiloride inhibits macropinocytosis by lowering submembranous pH and preventing Rac1 and Cdc42 signaling, J. Cell Biol. 188 (4) (2010) 547–563.
[28] P. Aleksandrowicz, A. Marzi, N. Biedenkopf, N. Beimforde, S. Becker, T. Hoenen, et al., Ebola virus enters host cells by macropinocytosis and clathrin-mediated endocytosis, J. Infect. Dis. 204 (Suppl 3) (2011) S957–S967.
[29] E. Sanchez-Ortiz, W. Cho, I. Nazarenko, W. Mo, J. Chen, L.F. Parada, NF1 regulation of RAS/ERK signaling is required for appropriate granule neuron progenitor expansion and migration in cerebellar development, Genes Dev. 28 (21) (2014) 2407–2420.
[30] L.J. Klesse, L.F. Parada, p21 ras and phosphatidylinositol-3 kinase are required for survival of wild-type and NF1 mutant sensory neurons, J. Neurosci. 18 (24) (1998) 10420–10428.
[31] B. Hegedus, B. Dasgupta, J.E. Shin, R.J. Emnett, E.K. Hart-Mahon, L. Elghazi, et al., Neurofibromatosis-1 regulates neuronal and glial cell differentiation from neuroglial progenitors in vivo by both cAMP- and Ras-dependent mechanisms, Cell Stem Cell 1 (4) (2007) 443–457.
[32] D.Y. Lee, T.H. Yeh, R.J. Emnett, C.R. White, D.H. Gutmann, Neurofibromatosis-1 regulates neuroglial progenitor proliferation and glial differentiation in a brain region-specific manner, Genes Dev. 24 (20) (2010) 2317–2329.
[33] S. Gupta, A.R. Ramjaun, P. Haiko, Y. Wang, P.H. Warne, B. Nicke, et al., Binding of ras to phosphoinositide 3-kinase p110alpha is required for ras-driven tumorigenesis in mice, Cell 129 (5) (2007) 957–968.
[34] D. Chaponis, J.W. Barnes, J.L. Dellagatta, S. Kesari, E. Fast, C. Sauvageot, et al., Lonafarnib (SCH66336) improves the activity of temozolomide and radiation for orthotopic malignant gliomas, J. Neuro Oncol. 104 (1) (2011) 179–189.
[35] F. Kanai, H. Liu, S.J. Field, H. Akbary, T. Matsuo, G.E. Brown, et al., The PX domains of p47phox and p40phox bind to lipid products of PI(3)K, Nat. Cell Biol. 3 (7) (2001) 675–678.
[36] S.S. Singh, A. Chauhan, H. Brockerhoff, V.P. Chauhan, Activation of protein kinase C by phosphatidylinositol 3,4,5-trisphosphate, Biochem. Biophys. Res. Commun. 195 (1) (1993) 104–112.
[37] D.N. Meijles, L.M. Fan, B.J. Howlin, J.M. Li, Molecular insights of p47phox phosphorylation dynamics in the regulation of NADPH oxidase activation and superoxide production, J. Biol. Chem. 289 (33) (2014) 22759–22770.
[38] M.T. Park, M.J. Kim, Y. Suh, R.K. Kim, H. Kim, E.J. Lim, et al., Novel signaling axis for ROS generation during K-Ras-induced cellular transformation, Cell Death Differ. 21 (8) (2014) 1185–1197.
[39] P. Ghoshal, B. Singla, H. Lin, D.M. Feck, N. Cantu-Medellin, E.E. Kelley, et al., Nox2-Mediated PI3K and cofilin activation confers alternate redox control of macrophage pinocytosis, Antioxidants Redox Signal. 26 (16) (2017) 902–916.
[40] K. Hirayama, M. Kobayashi, N. Yamaguchi, S. Iwabuchi, M. Gotoh, C. Inoue, et al., A case of renovascular hypertension associated with neurofibromatosis, Nephron 72 (4) (1996) 699–704.

[41] J. Oswald, S. Boxberger, B. Jorgensen, S. Feldmann, G. Ehninger, M. Bornhauser, et al., Mesenchymal stem cells can be differentiated into endothelial cells in vitro, Stem Cell. 22 (3) (2004) 377–384.
[42] A.C. Li, C.J. Binder, A. Gutierrez, K.K. Brown, C.R. Plotkin, J.W. Pattison, et al., Differential inhibition of macrophage foam-cell formation and atherosclerosis in mice by PPARalpha, beta/delta, and gamma, J. Clin. Investig. 114 (11) (2004) 1564–1576.
[43] D.M. Mosser, J.P. Edwards, Exploring the full spectrum of macrophage activation, Nat. Rev. Immunol. 8 (12) (2008) 958–969.
[44] J. Shi, Z. Wu, Z. Li, J. Ji, Roles of macrophage subtypes in bowel anastomotic healing and anastomotic leakage, J Immunol Res 2018 (2018) 6827237.
[45] J. MacMicking, Q.W. Xie, C. Nathan, Nitric oxide and macrophage function, Annu. Rev. Immunol. 15 (1997) 323–350.
[46] C.E. Arnold, C.S. Whyte, P. Gordon, R.N. Barker, A.J. Rees, H.M. Wilson, A critical role for suppressor of cytokine signalling 3 in promoting M1 macrophage activation and function in vitro and in vivo, Immunology 141 (1) (2014) 96–110.
[47] K.A. Jablonski, S.A. Amici, L.M. Webb, D. Ruiz-Rosado Jde, P.G. Popovich, S. Partida-Sanchez, et al., Novel markers to delineate murine M1 and M2 macrophages, PLoS One 10 (12) (2015) e0145342.
[48] J.F. Longo, S.M. Weber, B.P. Turner-Ivey, S.L. Carroll, Recent advances in the diagnosis and pathogenesis of neurofibromatosis type 1 (NF1)-associated peripheral nervous system neoplasms, Adv. Anat. Pathol. 25 (5) (2018) 353–368.
[49] F. Chang, L.S. Steelman, J.T. Lee, J.G. Shelton, P.M. Navolanic, W.L. Blalock, et al., Signal transduction mediated by the Ras/Raf/MEK/ERK pathway from cytokine receptors to transcription factors: potential targeting for therapeutic intervention, Leukemia 17 (7) (2003) 1263–1293.
[50] M.V. Recouvreux, C. Commisso, Macropinocytosis: a metabolic adaptation to nutrient stress in cancer, Front. Endocrinol. 8 (2017) 261.
[51] A.C. Hirbe, D.H. Gutmann, Neurofibromatosis type 1: a multidisciplinary approach to care, Lancet Neurol. 13 (8) (2014) 834–843.
[52] A.I. Ivanov, Pharmacological inhibition of endocytic pathways: is it specific enough to be useful? Methods Mol. Biol. 440 (2008) 15–33.
[53] Y. Egami, T. Taguchi, M. Maekawa, H. Arai, N. Araki, Small GTPases and phosphoinositides in the regulatory mechanisms of macropinosome formation and maturation, Front. Physiol. 5 (2014) 374.
[54] A. De Luca, M.R. Maiello, A. D'Alessio, M. Pergameno, N. Normanno, The RAS/RAF/MEK/ERK and the PI3K/AKT signalling pathways: role in cancer pathogenesis and implications for therapeutic approaches, Expert Opin. Ther. Targets 16 (Suppl 2) (2012) S17–S27.
[55] M. Maekawa, S. Terasaka, Y. Mochizuki, K. Kawai, Y. Ikeda, N. Araki, et al., Sequential breakdown of 3-phosphorylated phosphoinositides is essential for the completion of macropinocytosis, Proc. Natl. Acad. Sci. U. S. A. 111 (11) (2014) E978–E987.
[56] K. Bedard, K.H. Krause, The NOX family of ROS-generating NADPH oxidases: physiology and pathophysiology, Physiol. Rev. 87 (1) (2007) 245–313.
[57] W.K. Bessler, F.Z. Hudson, H. Zhang, V. Harris, Y. Wang, J.A. Mund, et al., Neurofibromin is a novel regulator of Ras-induced reactive oxygen species production in mice and humans, Free Radic. Biol. Med. 97 (2016) 212–222.
[58] S.A. Su, Y. Xie, Z. Fu, Y. Wang, J.A. Wang, M. Xiang, Emerging role of exosome-mediated intercellular communication in vascular remodeling, Oncotarget 8 (15) (2017) 25700–25712.